



Full length article

# Rethinking Lindemann criterion: A molecular dynamics simulation of surface mediated melting

Xue Fan<sup>a,b</sup>, Deng Pan<sup>c,\*</sup>, Mo Li<sup>b,\*</sup><sup>a</sup> School of Materials Science and Engineering, University of Shanghai for Science and Technology, Shanghai 200090, China<sup>b</sup> School of Materials Science and Engineering, Georgia Institute of Technology, Atlanta, GA 30332, United States<sup>c</sup> Materials Genome Institute, Shanghai University, 99 Shangda Road, Shanghai 200444, People's Republic of China

## ARTICLE INFO

## Article History:

Received 4 December 2019

Revised 5 May 2020

Accepted 5 May 2020

Available online 12 May 2020

## Keywords:

Melting  
Surface melting  
Self-diffusion  
Lindemann criterion

## ABSTRACT

Lindemann criterion has been the orthodox view for melting, and its interpretation of both the disordering process of the crystalline solids and formation of the liquid phases involved in melting extends to many other branches of science. However, an increasing number of works rebuke the universal criterion conceived by Lindemann in perfect bulk crystals. Here we examine the criterion in a more realistic setting of surface mediated melting from atomistic modeling. As a defect, surface helps mediating melting both on the surface and in the bulk. While this general relation is known, detailed mechanisms and atomic structural changes remain elusive, especially in relation to the Lindemann criterion. Our extensive molecular dynamics simulations show that in bcc Ta, the surface disorders first but still remains in crystalline state; and the bulk melts when the surface liquid layer forms and subsequently grows inside the bulk. The Lindemann parameter during the entire melting process remains a variable rather than a (universal) constant that supposedly predicts the onset of surface as well as the bulk melting. In addition, we observe surface diffusion and formation of correlated atomic chains and loops that are originated from the surface and permeate into the bulk crystals, causing the bulk to melt.

© 2020 Acta Materialia Inc. Published by Elsevier Ltd. All rights reserved.

## 1. Introduction

Melting is a phase transition where upon being heated, a solid melts into a liquid. However, this seemingly simple phenomenon turns out to be one of the most difficult to understand. Without the details of the atomic processes and mechanisms, melting is traditionally formulated using order parameter theories [1,2]. Either the structural quantities such as the structure factor commonly seen in diffraction experiments [3,4], or the bond orientational order parameter [5] or the atomic displacement in theories or modeling have been used as the order parameter. At the melting point, these quantities exhibit a finite change, indicating a first order phase transition. Among these theories, Lindemann criterion (LC) assumes a plausible mechanism that predicts the occurrence of melting when the mean atomic displacements (MADs) from the atomic vibration in the heated crystal reaches a critical value, i.e. the critical Lindemann parameter (LP) [6–8]. In particular, the critical LP is thought to be a universal value for crystals with the same atomic structure [6–14]. Due to its simplicity, this theory has since become the orthodox view to interpret melting in the past century. In addition, many concepts developed from the criterion, such as the critical mean atomic displacement and localization-to-delocalization transition in terms of

the atomic motion, become widely used, in particular in atomistic modeling, to describe the atoms involved in the solid to liquid/amorphous phase transitions [15,16].

Despite its popularity, the theory has been questioned constantly [17–19]. Among these works, we showed that contrary to Lindemann's proposal, the MAD does not uniquely predict the onset of the melting transition [15]. For example, in perfect bulk crystals, the dynamic MAD does reach the Lindemann value. However, instead melting into a liquid, the atoms in the crystals with the MAD larger than the Lindemann critical value do not change into liquid, but rather execute diffusional motion by hopping from lattice sites to lattice sites. The large atomic motion on the lattice does not cause melting as predicted by the Lindemann theory although they contribute greatly to the overall MAD or LP. Instead, these atoms form highly correlated atomic configurations in the form of the atomic chains and loops. Only when the number of these chains and loops reaches a certain level does melting occur at a higher temperature [15,16,20].

Perhaps the most important consequence of the new mechanism is that it rebukes the definition of the so-called liquid atoms in a heated crystal that have the MADs exceeding the value set by the LC. These atoms are neither liquid, nor liquid-like; they are still crystalline in nature, since their equilibrium, or time averaged atomic positions are still located on the crystalline lattices. Therefore, melting occurs not by forming large enough number of the "liquid-like atoms" as expected from the Lindemann theory; rather a crystal

\* Corresponding authors.

E-mail address: [mo.li@gatech.edu](mailto:mo.li@gatech.edu) (M. Li).

melts when the correlated atomic configurations in the form of chains and loops proliferate. The new finding points to new mechanisms of melting that was not anticipated in the LC. This is not surprising since the Lindemann theory only considers the *individual* atomic vibrational motion for the atoms away from the perfect crystalline lattice, and only the crystalline phase without the liquid is involved.

In addition, we know that in real life melting usually starts from the crystal surfaces. As a defect, surface helps mediating melting both on the surface and subsequently, in the bulk. This can be explained rather simply in thermodynamics: the free energy of the crystal with a free surface is slightly higher than that of the perfect crystal, or the bulk crystal without boundaries [21]. Therefore, when the free energy of the crystal crosses that of the liquid at increasing temperature, melting occurs at the surface with a lower melting point, or pre-melting, than the bulk melting temperature of a surface free crystal. While this general relation is known, detailed mechanistic processes and atomic structural changes remain elusive, especially in relation to the LC. As the atoms on the surface are relatively loosely bonded due to the reduced number of neighbors on the surface, it is easier for the surface atoms to move away from their lattice positions, which is the cause for pre-melting. The phenomenon of pre-melting has been observed from both experiments and simulations, as well as theories [22–29], however, the surface contribution to the Lindemann criterion and the underlying atomic mechanisms of melting is not sufficiently elucidated. For example, in most high angle diffraction experiments during crystal melting, the values of the Lindemann parameter obtained from the MADs include simultaneously the contributions from both the atoms on the surface and those from the bulk [30]. Since the surface only contributes a tiny portion to the total diffraction signal, its contribution to the Lindemann value cannot be measured, although melting in these crystals are originated from the surfaces. Small angle scattering can measure the contribution from the surface [31,32], but quantitative information about the atomic process and mechanisms including Lindemann parameter remains scant. As a result, many questions fundamental to our understanding of melting still remain unanswered. Here we list a few:

- In the thermodynamic explanation of surface melting, if a surface melts first via the surface with a much lower Lindemann value, should the bulk melting that follows occur also at a lower Lindemann value? In other words, if melting is dominated by surface melting, which is often casted in the relationship among the surface and interface energies,  $\gamma_h + \gamma_{sl} < \gamma_{sv}$ , where  $\gamma_{sv}$  is the original solid (s)-vapor (v) interface energy before the solid melts into liquid,  $\gamma_{sl}$  the solid-liquid (l) interface energy after a liquid phase forms on the surface, and  $\gamma_h$  the new liquid-vapor surface energy after the solid surface becomes a liquid. The relation says that the solid-liquid interface formation, or surface melting, is energetically favorable and once occurs would propagate to the bulk to cause the bulk melting. Therefore, the bulk melting is part of the surface melting. In this case, can we still use the LP obtained from the bulk crystals to predict melting that is caused by surface? Unfortunately, we should mention that it has been the common practice so far.
- Then how do the surface atoms change from the solid phase to a liquid phase? Do they follow the process predicted by Lindemann, i.e. via vibrating around their lattice positions first and then becoming liquid, or by other mechanisms, such as the atomic hopping on the (surface) lattice sites first and then forming correlated atomic chains and loops as seen in bulk crystalline solids [15,16]?
- And finally, how much does the surface atoms contributes to the measured Lindemann values, or whether does the LC still predict the surface mediated melting?

To answer these questions, we investigate the surface mediated melting from extensive molecular dynamics (MD) simulations on

bcc Ta. The reason to choose a bcc crystal will be explained below. As shown below, the choice of the bcc crystal does not limit our conclusions: We observed the same results in other structures including fcc [33]. Therefore, we only present the results for Ta. To give the reader an overview and a sense of significance of this work pertinent to the above questions, we summarize our results here before more technical details are introduced.

We observe that when heated, the crystal surface disorders first and then a liquid surface layer forms; and once the liquid layers forms, the bulk melting ensues as the result of the rapidly growing surface liquid phase into the bulk. The melting transition appears to be a gradual process via a layer-by-layer melting from the surface toward the bulk. Each of the melting crystal layers has a different Lindemann parameter, not a constant or any universal value. These results draw us to the conclusion that the Lindemann criterion does not, and should not, predict surface mediated melting. In addition, we found that along with the surface diffusion at the elevated temperature toward melting, correlated atomic chains and loops are generated on the surfaces that permeate into the bulk crystal. This observation points to possibly new mechanisms for surface mediated melting other than just the independent atomic thermal vibration. Since most melting occurs in crystals with surfaces, the applicability of the LC from these measurements is highly questionable. In addition, the LC fails to identify and remove the MADs contributed from the lattice diffusions in the bulk as well as on surface. In the past, these MADs from the lattice diffusion have been mistakenly used to define the liquid phase or “liquid-like” atoms. In the following, we shall give a detailed account of our investigation and results that support the above conclusions.

## 2. Methods

### 2.1. Simulation methods

In this work, we use bcc Ta as an example. The bcc structure has an open atomic packing that gives us several advantages. The first is that it is less anisotropic in surface density and energies, which gives as small as possible differences in melting mechanisms of surface mediated melting with different surfaces. In contrast, the strongly anisotropic fcc metals show (110) surface pre-melting while other surfaces exhibit either reconstruction or even superheating [34]. Therefore, with bcc Ta we can focus on the generic mechanisms of surface mediated melting, rather than the anisotropy related surface ordering and disordering. The second is that the more open bcc structure would likely tolerate more disordering caused by lattice vibration, which is shown by the already known larger values of the LP at melting. This would give us a larger temperature interval between surface and bulk melting for clear observation of the two. Hence we could identify and characterize the surface and bulk melting unambiguously.

To simulate melting and the related atomic-level properties, we use the classical molecular dynamics (MD) simulation implemented via the large-scale atomic/molecular massively parallel simulator (LAMMPS) [35]. Ta atoms interact with each other via an embedded atom method (EAM) interatomic interaction [36]. The interaction has been used in various occasions of bulk and surface melting [37,38]. To model the surface mediated melting, we arrange the atoms in a bcc structure but leave two surfaces exposed on two sides of the sample along the x direction. The atoms do not interact with each other across the surfaces, while along the other two directions parallel to the surfaces the atoms still retain the periodic boundary conditions. In this work, we investigate three typical surfaces, (100), (110) and (111). The system size ranging from 16,000 to 500,000 atoms are used to test the size effect. As the thermal fluctuations are inversely proportional to the sample size, smaller systems have slightly lower melting points. The difference, however, becomes negligible when

the number of atoms approaches above several thousand atoms. Since no significant size effects were found, we shall arrange the simulation cells for each of these samples with the three types of surfaces with 54,000, 48,000, and 36,000 atoms separately. The results reported from this work are primarily from these samples.

To implement heating, we use the isothermal-isobaric (NPT) ensemble MD method. The Noé-Hoover method [39,40] is used to control the temperature. The Newton equations of motion are solved numerically with a time step of 1 fs per step. Both gradual heating and isothermal method are used here. For the former, a constant heating rate of  $10^{11}$  K/s is used to heat the samples from 300 K until they melt at the melting points. Note that since the temperature  $T$  is linearly related to time  $t$  through the heating rate in gradual heating, the two are used interchangeably. For this reason, when applicable we plot both the temperature and time at the bottom and top of the figures. For isothermal case, the samples are heated with the same heating rate but kept at a designated temperature isothermally after. The atomic trajectories are collected for all atoms every 10 ps at which the temperature changes by about 1 K for analysis and calculation of structure and properties.

## 2.2. Characterization methods for melting

Experimental melting temperature for Ta is 3290 K [41]. In MD simulation, the melting point depend on the heating rate in the gradual heating case, the boundary condition, as well as the interatomic potentials used. The influence of these factors needs to be characterized in a self-consistent manner. For the bulk Ta without free surfaces, the melting point in the MD simulation is 3430 K [42] and with a (100) free surface, the bulk melting point is 3094 K, both with the heating rate at  $10^{11}$  K/s (see below). For the former, the bulk melting points are determined by locating the temperature at which the system volume or energy shows an abrupt change as melting is a first order phase transition. The equilibrium melting point is determined via monitoring the crystal-liquid interface motion [43,44] which is 3040 K for Ta as compared with the experimental one at 3290 K. Hence, the model system of Ta has a slightly lower melting point due to the interatomic interaction used. However, the trend of the melting behaviors is self-consistent and the conclusions we draw from the modeling will not be affected.

For systems with free surfaces, the melting transition is usually marked by the appearance of a so-called premelting on the surface [45–48] that occurs below the bulk melting temperature. As shown below, the “premelting” happens for Ta too. However, we will show that it is more a disordering process than an actual phase transition. Since the associated volume or energy change is small when the surface disordering occurs, we have to use various special methods to determine carefully this temperature and associated property change for this process and the subsequent bulk melting.

One is the mean square displacement (MSD),  $\overrightarrow{r}_i(t) - \overrightarrow{r}_i(0)$  for each atom  $i$  on the surface, as well as in the bulk. The MSD is the distance square between the position  $\overrightarrow{r}_i(t)$  at time  $t$ , or temperature  $T$ , and the position  $\overrightarrow{r}_i(0)$  at temperature  $T = 300$  K and the initial time  $t = 0$ . For a system at different time or temperature, the MSD is calculated by taking the average over the number of atoms,

$\Delta r^2(t) = \frac{1}{N} \sum_{i=1}^N |\overrightarrow{r}_i(t) - \overrightarrow{r}_i(0)|^2$ , where  $N$  can be the number of the surface or interior atoms, or the entire sample. Each of the choices gives the corresponding mean displacement on the surface, inside the sample, and the entire sample.

From the MSDs, we can calculate the Lindemann parameter  $\delta_L$  defined as the ratio of the root-mean-square displacement, or  $\Delta r(T)^{1/2}$ , divided by the average nearest neighbor distance,  $\bar{r}_{nn}(T)$  at the same temperature  $T$  for the surface as well as the bulk atoms.

Both the quantities,  $\Delta r(t)$ ,  $^{21/2}$  and  $\bar{r}_{nn}(T)$  can be obtained from the MD simulation directly and used to monitor the onset of disordering or melting on the surface and in the bulk. In particular, with the ability to monitor surface atoms, we can give a qualitative assessment of the Lindemann parameters contributed from a surface.

Since the surface takes a small fraction of the atoms in the sample, it is not easy to detect surface melting as for the bulk. We found nevertheless that this local “phase transition” can be sensitively detected by the non-Gaussian parameter [49,50]  $\alpha_2 = \frac{3\langle \Delta r^4 \rangle}{5\langle \Delta r^2 \rangle^2} - 1$ , where  $\langle \cdot \cdot \cdot \rangle$  can be obtained from the atomic displacement  $\Delta r$  discussed above, and  $\langle \cdot \cdot \cdot \rangle$  stands for time average in MD simulation. The Non-Gaussian parameter measures statistical heterogeneity of an underlying random variable. During heating of a crystal, the MSDs are homogeneous, or the displacement from each atom remains statistically the same by following a Gaussian distribution, hence the value of  $\alpha_2$  is zero. If certain atoms start to execute the displacements larger than other atoms, or non-Gaussian, such as in surface disordering, the value of  $\alpha_2$  starts to rise. Therefore, from the change of  $\alpha_2$ , we can capture sensitively the starting temperature of surface disordering and related melting processes.

Two more quantities are used to monitor the structural change during surface and bulk melting. One is the structural factor (SF) defined as  $S_i(k) = \langle \frac{1}{N^2} | \sum_{j=1}^N \exp(i\mathbf{k} \cdot \mathbf{r}_{ij})|^2 \rangle$ , where  $\mathbf{k}$  is the wave vector along the <110> directions in bcc structure,  $r_{ij}$  is the nearest neighbor pair distance centered at atom  $i$ , and  $j$  runs over all  $N$  nearest neighbors. The SF defined this way is connected to the specific diffraction peak with the wave vector  $\mathbf{k}$  from the more densely packed (110) plane in the bcc structure. Its rise and fall indicate the degree of structure ordering and disordering. The value of the  $S_i(k)$  is close to one in a perfect crystal and zero in liquid state. For bcc Ta the first eight nearest neighbors often come within the same distance as the six second nearest neighbors when temperature is high. For this case, we pick  $N = 14$  when we cannot distinguish the first and the second neighbors.

Note that since  $S_i(k)$  is a true structural “order parameter”, we use it to define whether an atom is a liquid atom if its value is below 0.2, or a crystalline atom if it is larger. The critical value of 0.2 is chosen based on the mean  $S(k)$  value at the crystal-liquid interface when a liquid coexists with a crystal Ta at the equilibrium melting point. This approach is different from the widely used criterion to define “liquid” atoms based on the Lindemann criterion (see more discussions on this topic later). We will show in this work that the latter is erroneous.

Another quantity for structural characterization is the bond orientational order (BOO) parameter defined as  $Q_n(i) = \langle \frac{1}{N} | \sum_{j=1}^N \exp(in\theta(ij)) | \rangle$ , where  $\theta(ij)$  is the bond angle formed by the  $i$  and  $j$  atom neighbor vectors  $\mathbf{r}_i$  and  $\mathbf{r}_j$ ,  $N$  is the number of the nearest neighbor atoms, and  $N = 4$  for (100) square lattice. We use the BOO parameter to detect the nature of the surface melting, i.e. whether or not melting is first order or continuous in terms of the orientational order [51,52]. For the latter, we employ another structural parameter, the two-dimensional radial distribution function (2DRDF), to detect the translational symmetry change in a surface during melting. The 2DRDF is obtained by first selecting the atoms within a slice on the surface with 1.65 Å in thickness, then using the relation,  $g(r, \theta) = \frac{n(r \sim r + \Delta r, \theta \sim \theta + \Delta \theta)}{A(r \sim r + \Delta r, \theta \sim \theta + \Delta \theta) \rho_0}$  to calculate the RDF, where  $A$  is the area of a surface region bounded between the radial distance  $r$  and  $r + \Delta r$  in the plane, and polar angle  $\theta$  and  $\theta + \Delta \theta$ ;  $n(r \sim r + \Delta r, \theta \sim \theta + \Delta \theta)$  is the number of atoms inside the slice, and  $\rho_0$  the mean atomic number density of the slice.

### 3. Results

#### 3.1. Surface mediated melting

When heated from 300 K to higher temperature, the bcc metal with (100) surfaces undergoes structural disordering, that is shown in Fig. 1 by the structural factor  $S(k)$ , Lindemann parameter  $\delta_L$ , and the non-Gaussian parameter  $\alpha_2$ . The continuously decreasing value of  $S(k)$  indicates the increasing structural disorder as atoms move away from their equilibrium lattice positions under thermal agitation. However, its magnitude abruptly drops to nearly zero at 3094 K, which is a typical sign for a first order melting transition. However, the sample averaged  $S(k)$  does not capture the surface disordering or melting that occurs in the first few surface layers, which can be done by the non-Gaussian parameter.

The non-Gaussian parameter,  $\alpha_2$ , captures the subtle change in the surface region. As shown in Fig. 1, the value of  $\alpha_2$  remains zero before but raises up suddenly at 1641 K. As a comparison,  $\alpha_2$  for the bulk Ta without surfaces starts to raise rapidly at about 2614 K [42]. The fast increasing  $\alpha_2$  value indicates the rising non-homogeneity in the atomic displacements, i.e. certain atoms move much further than the rest in some part of the sample at the given temperature. As discussed below, this unusual behavior is related to the surface disordering.  $\alpha_2$  reaches a peak value at 1911 K, then decreases subsequently at higher temperature, and approaches zero at the bulk melting point where the displacements of all atoms become homogeneous in a liquid phase.

The Lindemann parameter  $\delta_L$  taken from the entire sample increases with temperature. However, it remains below the Lindemann critical value  $\delta_L^* = 0.19$  [18] for the bulk bcc crystal. At 1641 K where surface starts to disorder, it reaches only about 0.16.  $\delta_L$  raises up beyond the Lindemann critical value above 2018 K before the sample melts (see inset in Fig. 1). Note that as we showed above, the entire samples melt into liquid at a much higher temperature, i.e. 3094 K, where the Lindemann parameter  $\delta_L$  is already orders of magnitude larger, which even appears as diverging (see Fig. 1).

These results tell us that like in the bulk sample without surfaces [15,42], in surface mediated melting the Lindemann criterion not only does not reach the predicted universal critical value at either surface melting or bulk melting, but even does not remain a constant to be qualified as a threshold. However, since we used the averaged

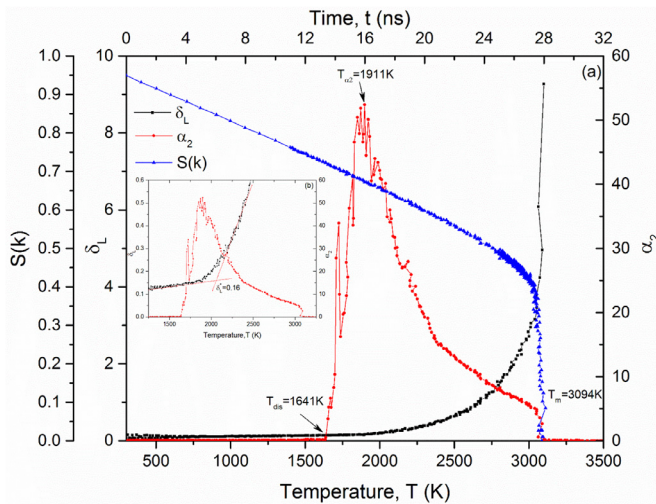


**Fig. 1.** The structural factor  $S(k)$ , Lindemann parameter  $\delta_L$ , and the non-Gaussian parameter  $\alpha_2$  for Ta with (100) surfaces versus temperature. The inset is the zoom-in of  $\delta_L$  and  $\alpha_2$  around 1641 K where surface disordering starts. Linear extrapolation is used to estimate the  $\delta_L$  values when the curve raises continuously. For gradual heating, the time elapse from 300 K is also plotted on the x-axis on the top of the figure.

value for  $\delta_L$  over the entire sample, one may argue that the surface contribution to  $\delta_L$  may still follow the Lindemann criterion on the surface. Because the surface contribution to  $\delta_L$  is small due to the small fraction of the number of the surface atoms as compared to these in the bulk, the averaged  $\delta_L$  over the entire sample cannot pick up the faint signal from the surface. Therefore, it is necessary to separately examine the surface contributions.

As seen above, the abrupt rise of the  $\alpha_2$  value at 1641 K indicates that the surface starts to disorder, or even possibly has undergone premelting. Unlike the Lindemann parameter  $\delta_L$ ,  $\alpha_2$  is not discriminated by the number of atoms on the surface. The larger MSD from the surface atoms is detected sensitively by  $\alpha_2$  despite the small number of atoms from the surface. To capture the surface mediated disordering or melting, we select a series of slices of atoms with the thickness  $d = 16 \text{ \AA}$  at different locations along the direction perpendicular to the surface, including the surface in the top slice. We then monitor the structure change directly in these slices to see how the surface disorder propagates inside. As temperature increases, melting should start at the top surface layer first and then move toward the interior. Hence the state of these atoms in each slice at different locations can tell us how the surface mediated disordering starts and gradually moves into the bulk.

We chose two typical temperatures, one corresponds to the peak of the  $\alpha_2$  value at 1911 K, and the other slightly below the bulk melting point at 3075 K where the  $\alpha_2$  value nearly approaches zero. As shown in Fig. 2(a), at 1911 K, the  $S(k)$  values of the surface atoms become smaller, indicating disordering, whereas the atoms inside the sample are fairly well ordered with large  $S(k)$  values typical for a well

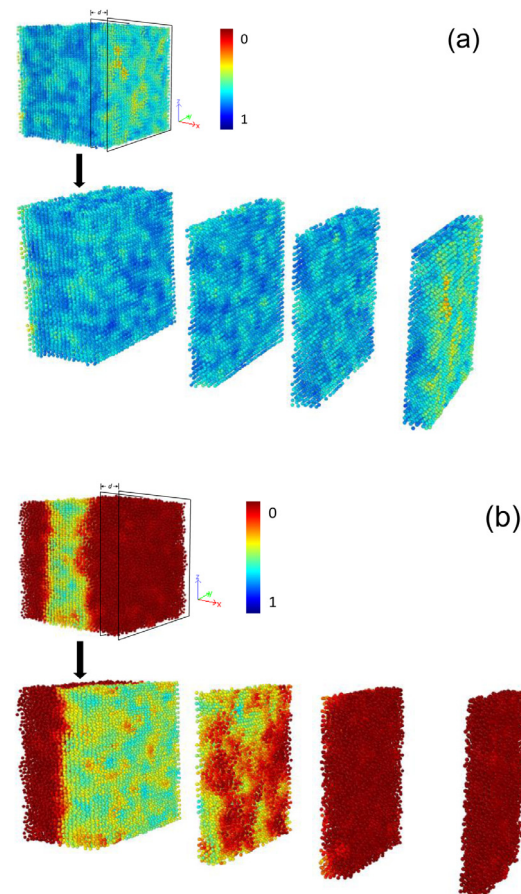


**Fig. 2.** The atomic configurations of the bcc Ta with a (100) surface at (a) 1911 K and (b) 3075 K. The color of the atoms is marked by the absolute values of the structure factor  $S(k)$  for each atom. The slices are cut at different locations from the surface with each slice thickness  $d = 16 \text{ \AA}$ .

ordered crystal. At 3075 K, Fig. 2(b) shows that the surface atoms are very disordered with the  $S(k)$  value hovering around 0.3, a value indicating severe structural disorder, and the disorder has already grown substantially into the interior of the samples. Clearly, the surface and subsurface disorder must lead to the large MSD in these regions, which results in highly heterogeneous MSD on surface regions at the lower temperature as shown by the  $\alpha_2$  value. But at higher temperature, the MSD becomes more homogeneous as the disorder spreads inside the sample, and at the same time there are larger atomic displacements emerging inside the sample. This trend is consistent with that of the  $\alpha_2$  values in Fig. 1.

The above results give us a clear sense of the sequence of the surface mediated melting in Ta: with the increasing temperature, the surface disorders first and subsequently the local disorder grows into the bulk. The final bulk melting occurs by following the growth of the surface mediated disordering. As we expected, there is a wide temperature range from 1641 to 3094 K, or about 25 ns in the gradual heating with the heating rate of  $10^{11}$  K/s, to complete this process in bcc Ta. The lower bound of the temperature marked by the rapid rise of  $\alpha_2$  sets the beginning of the surface disorder (Fig. 1(a)); the temperature corresponding to the peak of the  $\alpha_2$  represents the surface disordering (Fig. 1(b)) as well as the emergence of the disordering from the interior atoms with large MADs. The final bulk melting occurs as triggered by the growth or instability of the solid-liquid interface, which coincides with the thermodynamic instability condition of the interfaces formed in the surface regions (Fig. 2). Available experimental and simulation data on the interface energies for Ta close to the melting point indeed support this scenario: For Ta (100) surface,  $\gamma_{sl}=415 \text{ mJ/m}^2$  [53],  $\gamma_{lv}=2467 \text{ mJ/m}^2$  [54], and  $\gamma_{sv}=4050 \text{ mJ/m}^2$  [53], and hence, the condition  $\gamma_{lv} + \gamma_{sl} < \gamma_{sv}$  is met.

### 3.2. Atomic displacement and Lindemann parameter in surface mediated melting

The above results clearly show that the surface disorders first, and the disorder or possibly a liquid phase formed on the surface subsequently grows into the sample that leads to the final bulk melting. The inhomogeneity of the atomic motions at different locations of the sample at each temperature is picked up by  $\alpha_2$ . Then the pertinent question is how these highly heterogeneous atomic motions contribute to the atomic displacements and the related Lindemann parameters in different regions as melting proceeds from the surface. In the following, we shall find answers to this question.

As mentioned above, due to the presence of the surfaces where atoms have different bonding environment and are easy to be displaced under thermal agitation, surface disordering and melting should start with much lower MAD or Lindemann parameter  $\delta_L$ . However, as temperature goes higher, the surface atoms move further away from their lattice positions, leading to larger MAD and  $\delta_L$ , while inside the sample they still remain small. As the surface gets more disordered, the disordered region grows into the bulk. However, the surface contribution may not be measured easily, for example, using high angle diffraction or calorimetry. It is because the averaged sample value contains the overwhelmingly large contributions from the bulk. The surface contribution is likely missed out. This causes a serious inconsistency in the application of the Lindemann criterion: As we have known already that on the one hand, the bulk melting is caused by surface, and hence one should use the Lindemann critical value of the surface. But on the other hand, it is the bulk value that is measured and used to assess melting. Therefore, if no special techniques are used to probe the surface, such as the small angle scattering and surface ion channeling [55,56], the bulk MAD value measured in most experiments is used to measure melting. In the following, we shall examine the contributions from the surface, as well as the interior, to the MSD and the Lindemann parameter from the atomistic modeling.

The mean atomic displacements for surface and bulk atoms at each given temperature are obtained by first locating the number of the surface and the bulk atoms. The surface atoms are those that are from the top surface layer in the crystal. To check the variation of the results caused by this choice, we also follow the atoms on the subsurface layers that abut the surface and the bulk atoms by looking at the SF values of the atoms. Next, using the MADs of these atoms, we obtain their corresponding Lindemann parameters.

We define the value of  $\delta_L$  for the top surface layer as  $\delta_{s\_max}$  and the value for the layer next to the bulk as  $\delta_{s\_min}$ . At the same time, the mean value  $\delta_{surf}$  is taken from the entire surface regions. Indeed, as shown by Fig. 3(a), the surface atoms exhibit larger values of  $\delta_{surf}$  and more importantly,  $\delta_{surf}$  starts to rise up exactly at the surface disordering temperature at 1641 K, reaching a value between about 0.16~0.20 as shown in Fig. 3(b). However, in a stark contrast, the values of  $\delta_{bulk}$  at 1641 K for the interior of the sample remain well below the Lindemann's critical value of 0.19 predicted for the perfect bulk crystal.  $\delta_{bulk}$  only approaches this critical value at 2400 K, while the surface value of  $\delta_{surf}$  at this temperature has already been at least two orders of magnitude larger (Fig. 3(b)). At the bulk melting point at 3094 K, the value of  $\delta_{bulk}$  for the bulk is about 2, or 10 times larger than the predicted LC value for the perfect bcc crystals [11], and  $\delta_{surf}$  for the surface is larger than 10, or diverging.

Next, let us look at the weighted averages of the Lindemann parameter of the entire sample,  $\delta_L = x_{surf}\delta_{surf} + x_{bulk}\delta_{bulk}$ , where  $\delta_{surf}$  and  $\delta_{bulk}$  are the Lindemann parameters for the surface and bulk atoms,  $x_{surf}$  and  $x_{bulk}$  the atomic fraction of the surface and bulk atoms. In Fig. 4, we show the LP values, along with  $\delta_{surf}$  and  $\delta_{bulk}$ . One can see that the surface part,  $\delta_{surf}$ , increases with temperature but remains below the critical Lindemann value of 0.19; it shows unmistakably a rise only at 1694 K when the surface disordering starts, whereas that of the bulk  $\delta_{bulk}$  stays well below the critical Lindemann value until 2400 K. Most interesting is that the weighted average value of the LP  $\delta_L$  is nearly the same as that of the bulk  $x_{bulk}$ , due obviously to the large atomic fraction of the bulk atoms. Note that the above analysis is simply to demonstrate the inconsistency in application of the Lindemann criterion in the context of surface melting if only the sample averaged value is used. In real samples the surface fraction of atoms are negligible as compared to the bulk, which nullifies the surface contribution unless special techniques are employed [24].

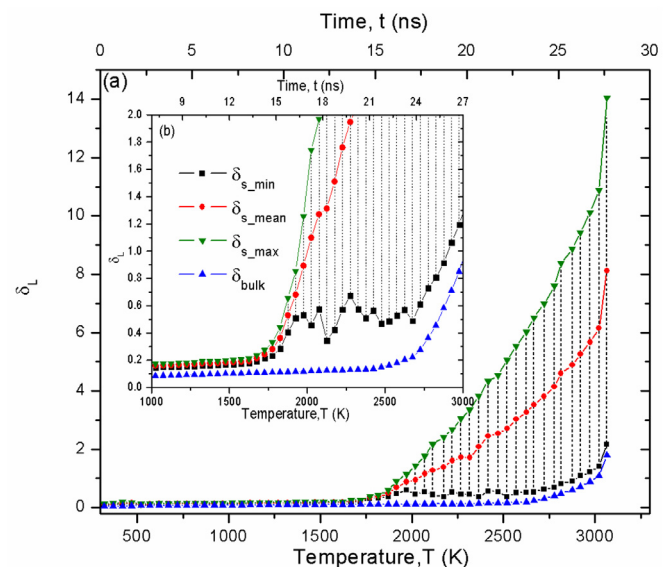


**Fig. 3.** The Lindemann parameters for the surface and the bulk versus temperature for a Ta with the (100) surface. The inset is the zoom-in of the  $\delta_L$ 's at the starting temperature of surface disordering around 1641 K.

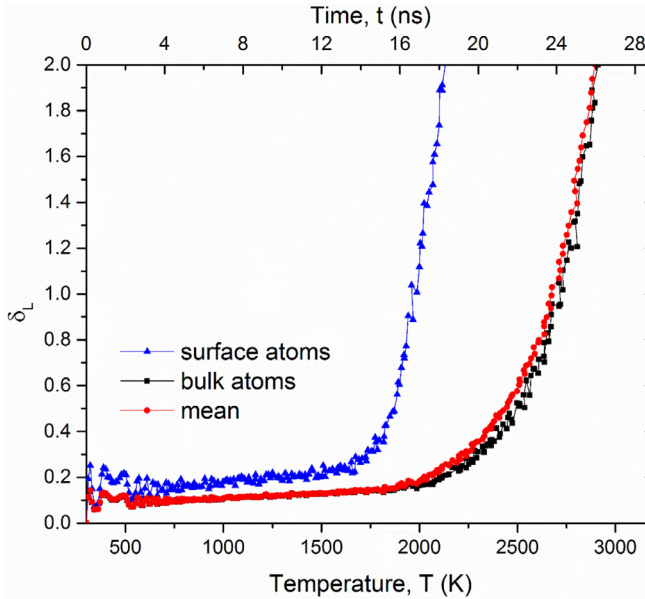


**Fig. 4.** The Lindemann parameters  $\delta_L$  versus temperature for Ta (100) for the surface atoms, the bulk crystalline atoms, and their weighted mean by the corresponding atomic fractions of the atoms.

The above arguments are further supported by the profiles of  $\delta_L(x)$  along the direction of the surface normal.  $\delta_L(x)$  is obtained in a series of slices with the thickness of  $1.65 \text{ \AA}$  for each at the location  $x$  cut from the sample paralleled to the surface. The MAD of the atoms in each slice is calculated at a given temperature, along with the mean nearest neighbor distance  $r_{nn}$ . From these quantities, one can obtain the local  $\delta_L(x)$  value at the location at  $x$  by taking the average of the  $\delta_L$  values of all atoms inside the slice. Fig. 5 shows the  $\delta_L(x)$  at different temperatures before the bulk melting point is approached, after which  $\delta_L(x)$  diverges. One can see clearly that at the temperature slightly below 1641 K, only the first slice on the top surface layer has the  $\delta_L(x)$  value approaching 0.2; at 2498 K, the five top layers have already have their  $\delta_L(x)$  values far larger than 0.2; and finally at 3039 K, slightly below the bulk melting point at 3094 K, the  $\delta_L(x)$  values in all layers, surface and bulk, become orders of magnitude larger than the Lindemann criterion value for a perfect bulk crystal without

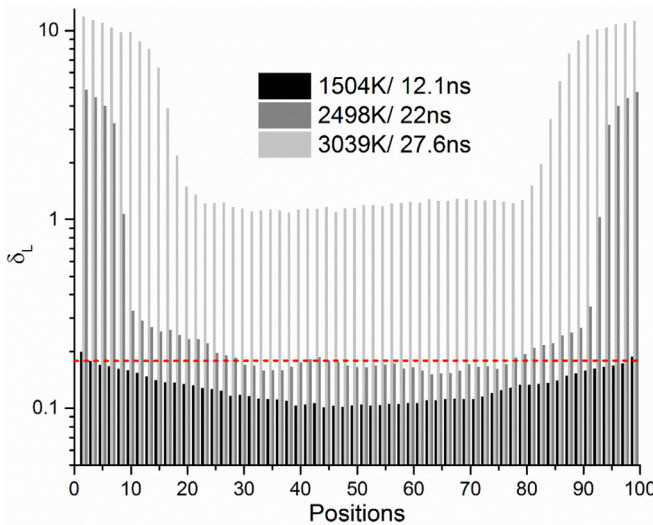


**Fig. 5.** The profiles of the Lindemann parameter inside each slices of the thickness of  $1.65 \text{ \AA}$  along the direction of the surface normal in a bcc Ta with the (100) surfaces at different temperatures. The red dash line shows the predicted Lindemann criterion for the perfect bulk crystal,  $\delta_L^* = 0.19$ .

surfaces. In light of these results, one can see clearly the irony in using the sample averaged LP in gauging bulk melting that is actually caused by the surface whose MAD is not included in the measured LP values from the bulk.

### 3.3. Structure characterization in surface mediated melting

Surface mediated melting is thought to start with a surface pre-melting which may even go through a possible second order transition, or wetting [24]. Our work here reveals that at least for bcc Ta, the so-called surface premelting is a gradual disordering process that spans a wide range of temperature from 1600 to 3094 K. During this temperature interval, the surface remains partially crystalline and partially liquid. In other words, the surface does not become completely liquid yet before the bulk melting point. Once the complete wetting occurs, the thermodynamic instability condition for the interface sets in, and the liquid layer becomes unstable and subsequently propagates to the rest of the sample. In other words, *surface and bulk melting occurs simultaneously*, not separately as thought before.

The above observation is also corroborated by the results from the quasi-2DRDF and BOO parameter within this temperature range. Fig. 6 is the 2DRDFs for the Ta surface with a (100) orientation at different temperatures. One can see that the square lattice structure of the (100) surface persists and is distinctly visible up to 2919 K, only less than 100 K below the bulk melting point. At 3075 K, slightly above the melting point, the crystalline structure disappears completely. The 2DRDF shows that the surface retains the crystalline structure until the bulk melting point is approached, which indicates a typical first order transition for the surface mediated melting.

Fig. 7(a) is the BOO parameter with respect to the increasing temperature obtained from the entire sample as well as in the layers parallel to the surface at different locations in the sample including the surface. Since the (100) surface has the symmetry of a square lattice, we use  $Q_4$  for BOO. One can see clearly that in general all  $Q_4$  values decrease with the increasing temperature, meaning the decreasing orientational order. However, the value of  $Q_4$  on the top surface layer  $a$  departs abruptly from the trend of those in other layers inside the sample and drops to lower values starting at 1600 K where we know that the surface disordering occurs at the temperature. The  $Q_4$  at the interior locations, layer  $b$ ,  $c$ , and  $d$ , keeps decreasing with the increasing temperature monotonically but remains in the level above 0.7, or a fairly well ordered state, until the bulk melting point at 3094 K. In addition, the top surface layer  $a$  as well as the subsurface layer  $b$ , however, has a faster decreasing trend in  $Q_4$ , and at the bulk melting point, plunges to 0.2, a severely disordered state, albeit crystalline. The sample mean  $Q_4$  value follows the general trend of those inside the sample and also shows an abrupt drop at the bulk melting point. We would like to remind the reader once again that if one uses the mean BOO value to evaluate melting of the entire sample as done with the MAD, one will not be able to see the larger surface disordering as it is weighted out by the small number of surface atoms. The results from the BOO parameter tell us that while the translational order is compromised, the surface goes through an orientational disordering also but remains crystalline, and finally becomes liquid at the bulk melting point, as a first order phase transition. Note that although the surface disordering results in a smaller BOO value for the surface layer(s) and their smaller drop at the bulk melting point, the finite change characteristic of a first order phase transition is still preserved.

To further check the possible continuous melting on the surface, the BOO correlation function for  $Q_4$ ,  $C_T(r) = \left[ \frac{1}{\pi r^2 N} \left( \sum_{i=1}^N \sum_{j \neq i}^N |Q_4(r_i)| * |Q_4(r_j)| \delta(r - r_{ij}) \right) \right]$ , is calculated for the atoms in the surface layer. Fig. 7(b) shows three correlation functions at the room temperature (300 K), the

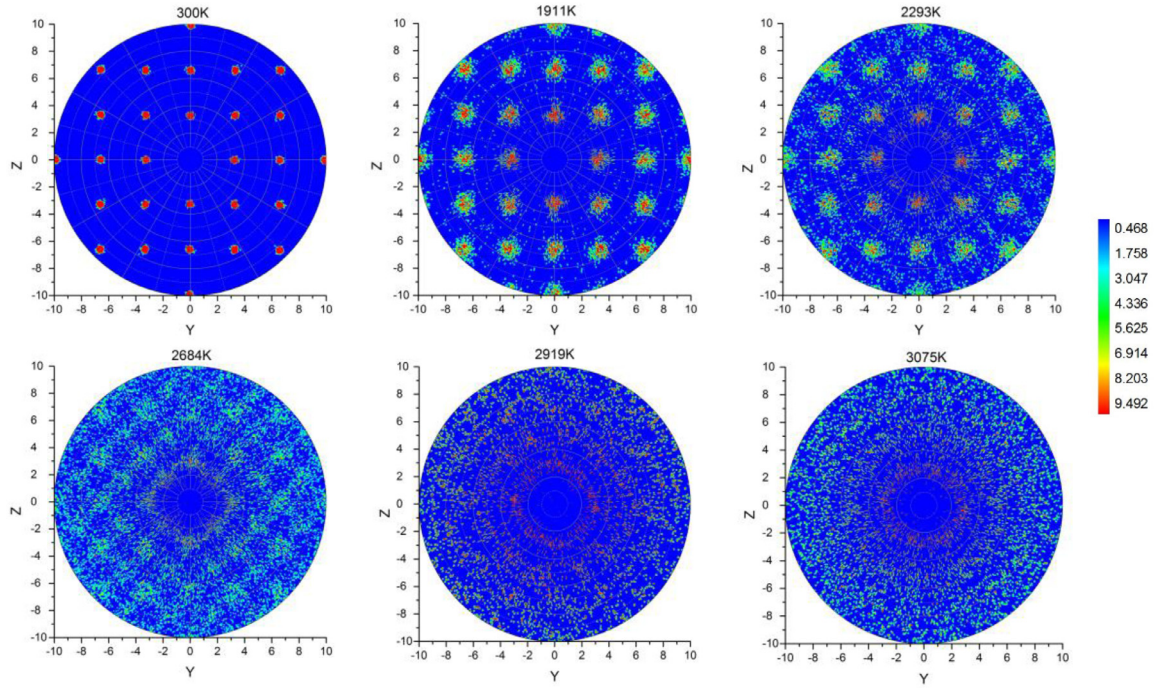


**Fig. 6.** The quasi 2DRDFs for a bcc Ta with the (100) surfaces at different temperatures. The scale bar marks the peak height of the 2DRDFs.

temperature slightly higher than the surface disordering temperature (1755 K), and slightly below the bulk melting temperature (3075 K). The correlation functions show that certain orientational order persists until the bulk melting after the surface disordering occurs at about 1600 K.

Combining the BOO with the information from the 2DRDF, we can conclude that the so-called pre-melting transition on the Ta surface is simply a disordering process that does not lead to complete melting or wetting until the bulk melting point is approached. In other words, *the surface melting appears in synchronization with the bulk melting as a first order phase transition*.

#### 3.4. Melting with other surfaces

As mentioned in the Introduction, bcc crystals have smaller anisotropy than the close-packed structures such as fcc and hcp crystals. This property is reflected in the surface mediated melting with different surfaces. Besides the (100) surface shown above, we examined Ta crystals with other two typical surfaces, i.e. the (110) and (111) surfaces. The results remain qualitatively the same. For this reason, we only give a brief summary of the results here.

Similar to Fig. 1, Fig. 8(a) shows the structure factor, Lindemann parameter and non-Gaussian parameter for bcc Ta with the three surface orientations as a function of temperature. The values of  $S(k)$  for the three samples decrease in the similar fashion with the increasing temperature and show abrupt drops, the sign of the first order melting, at 3082 K, 3094 K, and 3115 K for (111), (100), and (110) surfaces respectively, which are close to the corresponding experimental melting temperatures [41]. The melting points are in the order of (110)>(100)>(111), which is clearly related to the atomic number density in each surface: The (110) surface is the most densely packed surface in the bcc crystal with the packing density  $\frac{1}{a^3}$ ,  $a = 3.3058\text{\AA}$ , whereas  $\frac{1}{a^3}$  for (100), and  $\frac{0.58}{a^3}$  for (111) surfaces, here  $a$  is the lattice parameter.

The non-Gaussian parameter  $\alpha_2$  in Fig. 8(a) shows the same trend of surface disordering: The values of  $\alpha_2$  raise up at 735 K, 1641 K, and 2075 K for (111), (100) and (110) surfaces, respectively. This indicates that the atomic disordering occurs earlier in the more loosely packed (111) surface, then (100), and lastly, the most densely packed (110)

surface. While the  $\alpha_2$  values of the (100) and (110) surfaces exhibit a singular peak at 1911 K and 2342 K, the (111) surface shows two stages, one at 800 K and the other at 1735 K. The first peak at 800 K is related to the surface reconstruction on the more open (111) surface at low temperature [57] and the second at 1735 K is from the surface disordering.

The Lindemann parameters are shown in Fig. 8(a) and (b). Once again, the loosely packed (111) surface shows larger amplitude in vibrations than the (110) and (100) surfaces and thus larger dynamic MSD. Hence, the Lindemann parameter of the sample with the (111) surface raises up more with the increasing temperature than those of the (100) and (110) surfaces. As a result, the corresponding Lindemann parameter is  $\delta_L=0.13$ , 0.16 and 0.37 respectively for the (110), (100), and (111) surfaces. The departure occurs from the linear trend in  $\delta_L$  at low temperature; the largest departure in the  $\delta_L$  occurs for (111) surface. Note here that we use the interceptions of the two straight lines for the  $\delta_L$  at the low and high temperatures to approximate the Lindemann values (Fig. 8(b)). At the bulk melting points, one can see that the  $\delta_L$  for all three cases are orders of magnitude larger than the predicted Lindemann universal value (0.19) for the perfect bcc bulk crystal.

As in Fig. 4, in Fig. 8(c) we show the surface, interior and the weighted Lindemann parameters for the three samples. Once again we see the same trend for the three cases, that is, the surface atoms show the largest  $\delta_L$ , or disorder, at lower temperature, and the interior has nearly the same  $\delta_L$  values for all samples.

## 4. Discussions and conclusions

The description of the structural transition from the ordered crystal to disordered liquid has been dominated in the past century by the thinking originated from Lindemann. It predicts melting or liquid phase formation when the magnitude of the atomic dynamic vibration reaches a universal constant. In other words, the atoms that have the dynamic mean square displacement larger than the Lindemann critical value become liquid. We show in this work that both the concepts, the Lindemann universal criterion and the definition of liquid atoms, are riddled with questions, and worse, misunderstanding. These questions

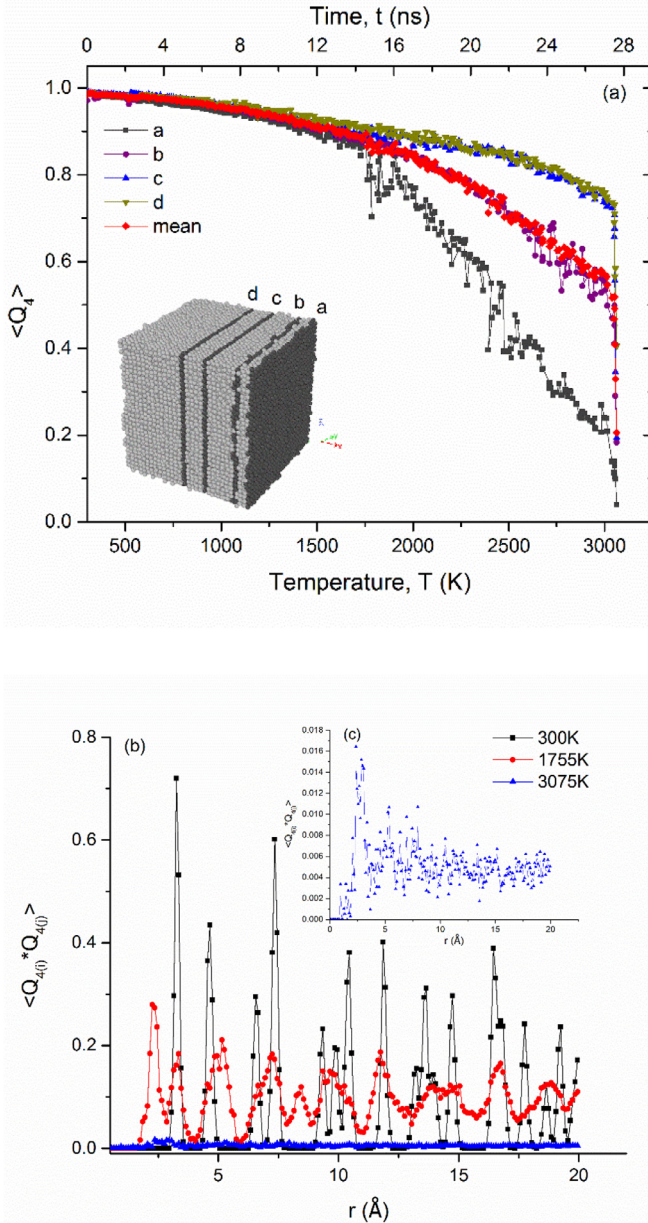


**Fig. 7.** (a) The BOO parameters in different layers parallel to the surface versus temperature in the bcc Ta with (100) surfaces. The inset shows the location of the layers (a, b, c and d). Each layer has the thickness of 3.5 Å. Layer a is the top surface layer. The average BOO parameter over the entire sample is also shown as a comparison. (b) The correlation functions of the BOO parameter  $Q_{4(r)}$  at different temperatures below the bulk melting temperature. The correlation function of highest temperature 3075 K is enlarged and shown as the inset (c).

are fundamental to the mechanistic understanding of not only melting but a large class of phase transformations involving ordered to disordered phases.

Our early work in perfect bulk fcc and bcc crystals [15,42] shows that the Lindemann parameter in general does not predict the onset of melting, although it captures the general trend of thermal-agitated disordering in the crystals. In the more realistic surface mediated melting as shown here, we see that neither the surface nor the bulk melting was predicted by the criterion, that is, the transition does not happen at a constant value of the LP. In the surface mediated melting, the situation is even complex – the values of the LPs are variables at different layers from the surface and at different temperatures. The nature

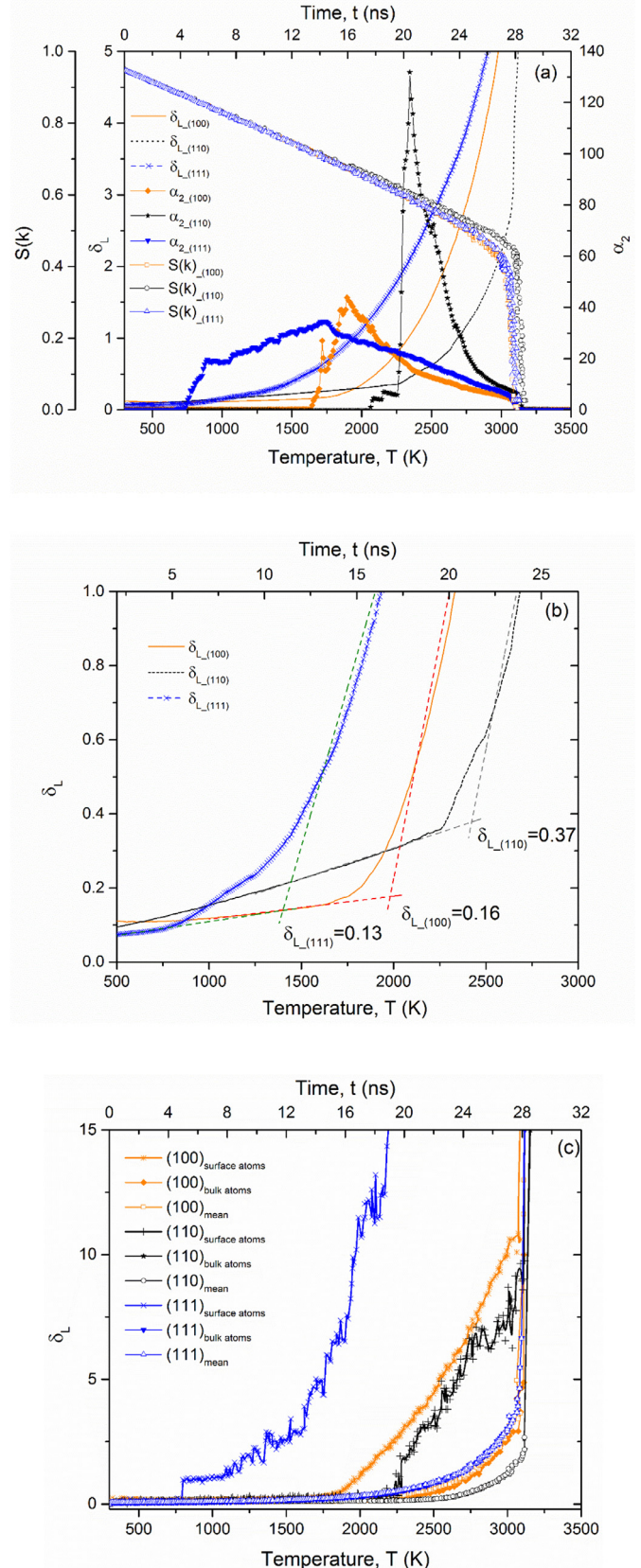


**Fig. 8.** (a) The structural factor  $S(k)$ , Lindemann parameter  $\delta_L$ , and the non-Gaussian parameter  $\alpha_2$  for Ta with (100), (110) and (111) surfaces versus temperature. The zoom-ins of the  $\delta_L$ 's are shown in (b). (c) The Lindemann parameters  $\delta_L$  versus temperature for the surface, the interior, and their weighted mean by the atomic fractions. The blue color is for (111) surface sample, orange for (100), and black for (110) surface.

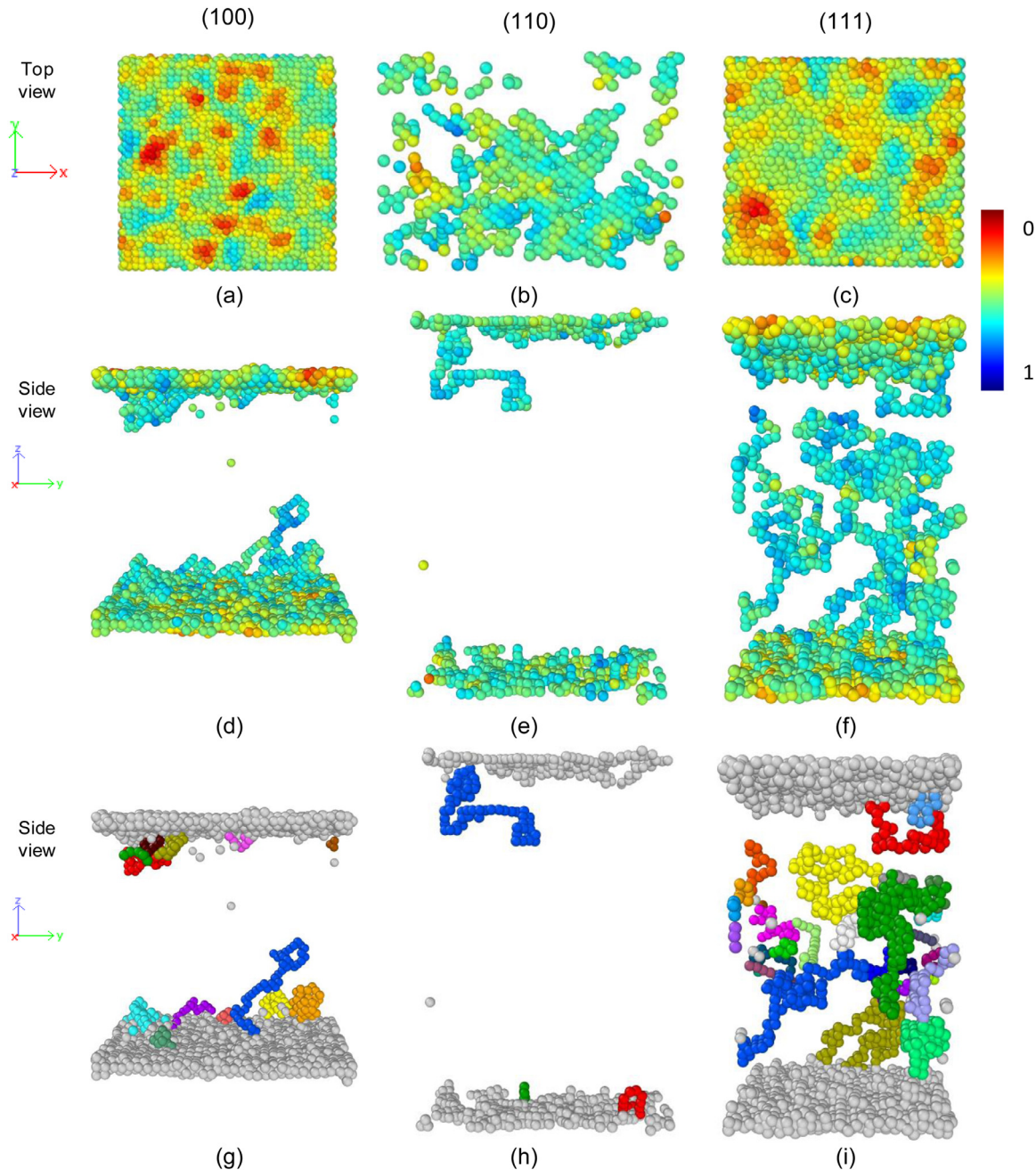


**Fig. 9.** The extended atomic configurations of the chains and loops that still execute the correlated diffusive atomic motion on crystal lattices for the bcc Ta with the (100), (110), and (111) surfaces at  $T = 2366$  K for the top view (a), (b), and (c), side view (d), (e), and (f). The color scheme used in (a)–(f) is based on the value of the structure factor (see the side bar for the color scheme). And the different chains and loops are colored differently to distinguish them (g), (h), and (i).

of the varying LPs makes it impossible to set up any “threshold”, not to mention “universal” criterion, to predict melting.

Some has argued that the failure is because the Lindemann criterion considers only one phase, the crystals, while a comprehensive theory should consider both the crystal and liquid. We need to point out that the use of MSD itself in predicting melting may be inappropriate to begin with. Firstly, the MSD remains meaningless to represent disorder in liquid state; therefore, even one considers the liquid phase in a more general theory of melting, the order parameter, i.e. the MDS, should not be used in the Lindemann type of theory. Secondly, we observe that the bulk melting of a crystal is caused by the surface disordering and the subsequent propagation of the disordering into the bulk. This mechanism has been known for quite some time, but many basic concepts remain either unexplored or misled, in particular the contributions to the Lindemann parameter from the

MAD from the surface and the bulk. Indeed, we found that the mean atomic displacement or the Lindemann parameter measured from the entire sample does not capture the melting mediated from the surface due to the small contribution from the surface. In addition, a large part of the MSD comes from the correlated atomic diffusion. The correlated lattice diffusion happens on the crystalline lattice at the temperature where the Lindemann predicts melting [15,42]. In other words, when the atomic displacement becomes large enough at high temperature, instead of jumping out of their lattice sites to form a liquid phase, the atoms execute highly correlated diffusional motion by landing on the crystal lattices. In perfect bulk crystals, we first discovered the atomic chains and loops that are engaged in the diffusional motion [15,42]. These correlated atomic motion contributes to the mean atomic displacement, and thus to Lindemann parameter. But they do not show crystal disorder toward liquid phase formation.

Ironically, these displacements are still counted into the Lindemann parameter. And the worst, one may mistake these atoms that still move on the crystal lattices as “liquid-like” or in the liquid phase.

In the case of the surface mediated melting, we found the same mechanisms in action. Fig. 9 is the snapshots of the extended atomic configurations of chains and loops in bcc Ta with (100), (110), and (111) free surfaces at temperatures close to the bulk melting points. In other words, the correlated atomic motion still occurs in surface melting. To prove that the atoms in these configurations are still crystal- or solid-like atoms, we color the atoms in the chains and loops with their corresponding values of the atomic structure factor  $S(k)$ : The more disordered the atoms are, the smaller the  $S(k)$  values that are colored with red color. One can see in Fig. 9(a)–(f) that indeed, the atoms in these extended configurations have the values of the structure factor well within the crystalline range, except these on the surfaces, that is, these atoms in the chains and loops undergoing diffusional motion are still in crystalline state. More details of the formation and dynamic properties of these extended atomic configurations will be given in a separate publication.

In summary, in this work we show a more realistic scenario of melting and the related Lindemann criterion in the surface mediated melting of the bcc Ta crystals. We demonstrate that melting is indeed generated from the free surfaces by first forming a thin liquid layer and then propagates to the interior of the bulk, and both the surface and bulk melting occurs synchronously as predicted by the thermodynamic conditions among the interface energies. We also found new atomistic mechanisms of surface mediated melting through formation of extended atomic configurations, i.e. chains and loops originated from the sample surface.

Perhaps the most noticeable is our observation of an irony related to the Lindemann criterion: On the one hand, the bulk melting is caused by the surface melting but the surface MSDs are not measured and used to gauge melting; and on the other hand, we insist using the MSD measured from the bulk to predict melting that is caused by surface. The new results and insights obtained from this work challenges the melting theory and the misunderstanding. We hope that this work will provide a needed help for development of new understanding of melting.

## Declaration of Competing Interest

None

## Acknowledgement

M.L. would like to acknowledge the support provided by the National Thousands Talents Award of China. X.F. would like to thank the support from the project of “Highland Disciplines of Shanghai Higher Education” supported by Shanghai Municipal Education Commission.

## Supplementary materials

Supplementary material associated with this article can be found in the online version at doi:[10.1016/j.actamat.2020.05.013](https://doi.org/10.1016/j.actamat.2020.05.013).

## References

- [1] G.H. Wannier, Melting as an order-disorder transition, *J. Chem. Phys.* 7 (1939) 810–817.
- [2] J.E. Lennard-Jones, A.F. Devonshire, Critical and co-operative phenomena. IV. A theory of disorder in solids and liquids and the process of melting, *Proc. Roy. Soc. (Lond.) A170* (1939) 464.
- [3] H. Olbrich, H. Ruppertsberg, S. Steeb, Experimental determination of the form and structure factor of Molten Lithium, *Z. Naturforsch.* 38a (1983) 1328–1336.
- [4] A. Alatas, A.H. Said, H. Sinn, G. Bortel, M.Y. Hu, J. Zhao, C.A. Burns, E. Burkert, E.E. Alp, Atomic form-factor measurements in the low-momentum transfer region for Li, Be, and Al by inelastic x-ray scattering, *Phys. Rev. B* 77 (2008) 064301.
- [5] J.S.v. Duijneveldt, D. Frenkel, Computer simulation study of free energy barriers in crystal nucleation, *J. Chem. Phys.* 96 (1992) 4655–4668.
- [6] V.A. Lindemann, Über die Berechnung molekulärer Eigenfrequenzen, *Phys. Z.* XI (1910) 609–612.
- [7] J.J. Gilvarry, The Lindemann and Grüneisen laws, *Phys. Rev.* 102 (1956) 308–316.
- [8] J.-P. Hansen, Phase Transition of the Lennard-Jones System. II. High-temperature limit, *Phys. Rev. A* 2 (1970) 221–230.
- [9] R.W. Cahn, Crystal defects and melting, *Nature* 273 (1978) 491–492.
- [10] F.H. Stillinger, T.A. Weber, Lindemann melting criterion and the Gaussian core model, *Phys. Rev. B* 22 (1980) 3790–3794.
- [11] S.A. Cho, Role of lattice structure on the Lindemann fusion theory of metal, *J. Phys. F Met. Phys.* 12 (1982).
- [12] Z.H. Jin, P. Gumbsch, K. Lu, E. Ma, Melting mechanisms at the limit of superheating, *Phys. Rev. Lett.* 87 (2001) 055703.
- [13] S.-N. Luo, A. Strachan, D.C. Swift, Vibrational density of states and Lindemann melting law, *J. Chem. Phys.* 122 (2005) 194709.
- [14] Q.S. Mei, K. Lu, Melting and superheating of crystalline solids: from bulk to nanocrystals, *Prog. Mater. Sci.* 52 (2007) 1175–1262.
- [15] X.M. Bai, M. Li, Ring-diffusion mediated homogeneous melting in the superheating regime, *Phys. Rev. B* 77 (2008).
- [16] H. Zhang, M. Khalakhal, Q. Liu, J.F. Douglas, String-like cooperative motion in homogeneous melting, *J. Chem. Phys.* 138 (2013) 12A538.
- [17] V.G. Chudinov, R.M.J. Cotterill, V.V. Andreev, Possible Mechanism for the Solid-Liquid Phase Transition in H.C.P. and B.C.C. Structure, *Phys. Stat. Sol.* 122 (1990) 187.
- [18] E.J. Meijer, D. Frenkel, Melting line of Yukawa system by computer simulation, *J. Chem. Phys.* 94 (1991) 2269–2271.
- [19] C. Chakravarty, P.G. Debenedetti, F.H. Stillinger, Lindemann measures for the solid-liquid phase transition, *J. Chem. Phys.* 126 (2007) 204508.
- [20] J. Sprakler, A. Zaccione, F. Spaepen, P. Schall, D.A. Weitz, Direct observation of entropic stabilization of bcc crystals near melting, *Phys. Rev. Lett.* 118 (2017) 088003.
- [21] J.W. Gibbs, On The Equilibrium of Heterogeneous Substances, in: *transactions of the connecticut academy of arts and sciences*, New Haven (1876) 108–249.
- [22] M. Bienfait, Surface premelting of CH<sub>4</sub> thin films, *Europhys. Lett.* 4 (1987) 79–84.
- [23] M. Bienfait, J.M. Gay, Surface premelting of thin films of methane, *Surf. Sci.* 204 (1988) 331–344.
- [24] J.G. Dash, *Surf. Melt. Contemp. Phys.* 30 (1989) 89–100.
- [25] H.a.M.M. Hakkinen, Computer simulation of disordering and premelting of low-index faces of copper, *Phys. Rev. B* 46 (1992) 1725–1742.
- [26] W. Theis, K. Horn, Surface premelting in Al(110) observed by core-level photo-emission, *Phys. Rev. B Condens. Matter.* 51 (1995) 7157–7159.
- [27] F.L. Tang, X.G. Cheng, W.J. Lu, W.Y. Yu, Premelting of Al nonperfect (111) surface, *Phys. B Condens. Matter.* 405 (2010) 1248–1252.
- [28] B. Li, F. Wang, D. Zhou, Y. Peng, R. Ni, Y. Han, Modes of surface premelting in colloidal crystals composed of attractive particles, *Nature* 531 (2016) 485–488.
- [29] J. Daeges, H. Gleiter, J.H. Perepezko, Superheating of metal crystals, *Phys. Lett. A* 119 (1986) 4.
- [30] L. Pedemoni, G. Bracco, R. Beikler, E. Taglauer, A. Robin, W. Heiland, A low-energy ion scattering study of Al(110) surface melting, *Surf. Sci.* 532–535 (2003) 13–18.
- [31] J.W. Frenken, J.F. van der Veen, Observation of surface melting, *Phys. Rev. Lett.* 54 (1985) 134–137.
- [32] J.F.V.D. Veen, J.W.M. Frenken, Dynamics and melting of surfaces, *Surf. Sci.* 178 (1986) 382–395.
- [33] R. Kojima, M. Susa, Surface melting of copper with (100), (110), and (111) orientations in terms of molecular dynamics simulation, *High Temp. High Press.* 34 (2002) 639–648.
- [34] K.C. Prince, U. Breuer, H.P. Bonzel, Anisotropy of the order-disorder phase transition on the Pb(110) surface, *Phys. Rev. Lett.* 60 (1988) 1146–1149.
- [35] S. Plimpton, Fast parallel algorithms for short-range molecular dynamics, *J. Comput. Phys.* 117 (1995) 1–19.
- [36] R. Ravelo, T.C. Germann, O. Guerrero, Q. An, B.L. Holian, Shock-induced plasticity in tantalum single crystals: interatomic potentials and large-scale molecular-dynamics simulations, *Phys. Rev. B* 88 (2013).
- [37] C.M. Liu, C. Xu, Y. Cheng, X.R. Chen, L.C. Cai, Melting curves and structural properties of tantalum from the modified-Z method, *J. Appl. Phys.* 118 (2015) 235901.
- [38] C.M. Liu, C. Xu, Y. Cheng, X.R. Chen, L.C. Cai, The effect of vacancies on melting properties of tantalum via molecular dynamics simulations, *Appl. Phys. A* 122 (2015) 22.
- [39] S. Nosé, A unified formulation of the constant temperature molecular dynamics methods, *J. Chem. Phys.* 81 (1984) 511–519.
- [40] W.G. Hoover, Canonical dynamics: equilibrium phase-space distributions, *Phys. Rev. A* 31 (1985) 1695–1697.
- [41] A.M. James, M.P. Lord, Macmillan's Chemical and Physical Data (1992).
- [42] X. Fan, D. Pan, M. Li, Melting of bcc crystal Ta without the Lindemann criterion, *J. Phys. Condens. Matter.* 31 (2019) 095402.
- [43] J.R. Morris, C.Z. Wang, K.M. Ho, C.T. Chan, Melting line of aluminum from simulations of coexisting phases, *Phys. Rev. B* 49 (1994) 3109–3115.
- [44] J.R. Morris, X. Song, The melting lines of model systems calculated from coexistence simulations, *J. Chem. Phys.* 116 (2002) 9352–9358.

- [45] F.D. Di Tolla, E. Tosatti, E. Ercolessi, Interplay of melting wetting overheating and faceting on metal surfaces theory and simulation, Monte Carlo and Molecular Dynamics of Condensed Matter Systems, SIF, Bologna, 1996, pp. 347–398.
- [46] M. Polcik, L. Wilde, J. Haase, Partial order of the quasiliquid during surface melting of Al(110), Phys. Rev. Lett. 78 (1997) 491–494.
- [47] V. Jahangir, R. Riahiifar, M. Sahba Yaghmaee, A thermodynamic model for predicting surface melting and overheating of different crystal planes in BCC, FCC and HCP pure metallic thin films, Thin Solid Films 603 (2016) 294–302.
- [48] V. Pontikis, S. Sivarajan, Surface Roughening, Reference Module in Materials Science and Materials Engineering, Elsevier, 2017.
- [49] W. Kob, S.C. Glotzer, Dynamical heterogeneities in a supercooled Lennard-Jones liquid, Phys. Rev. Lett. (1997) 79.
- [50] A. Rahman, Correlations in the motion of atoms in liquid argon, Phys. Rev. 136 (1964) A405–A411.
- [51] P.J. Steinhardt, D.R. Nelson, M. Ronchetti, Bond-orientational order in liquids and glasses, Phys. Rev. B 28 (1983) 784–805.
- [52] D.M. Herlach, T. Palberg, I. Klassen, S. Klein, R. Kobold, Overview: experimental studies of crystal nucleation: metals and colloids, J. Chem. Phys. 145 (2016) 211703.
- [53] Q. Jiang, H.M. Lu, Size dependent interface energy and its applications, Surf. Sci. Rep. 63 (2008) 427–464.
- [54] H.M. Lu, Q. Jiang, Surface tension and its temperature coefficient for liquid metals, J. Phys. Chem. B 109 (2005) 15463–15468.
- [55] H. Dosch, T. Höpfer, J. Peisl, R.L. Johnson, Synchrotron X-Ray Scattering from the Al(110) surface at the onset of surface melting, Europhys. Lett., 15 (1991) 527–533.
- [56] K. Pussi, J. Vuorinen, M. Lindroos, H.I. Li, J.D. Howe, K.J. Hanna, R.D. Diehl, P.K. Bandyopadhyay, Temperature dependent LEED study of Pb{111}, Surf. Sci. 603 (2009) 2759–2763.
- [57] V.I. Zubov, I.V. Mamontov, The microscopic theory of the surface properties of anharmonic crystals the (110) and (111) surface of bcc crystal, Int. J. Mod. Phys. B 6 (1992) 221–249.